Clim Dyn (2018) 51:1363–1373
DOI 10.1007/s00382-017-3959-4

Changes in the East Asian summer monsoon rainfall under global warming: moisture budget decompositions and the sources of uncertainty

Shijie Zhou[1,3] · **Gang Huang**[1,2,3] · **Ping Huang**[1,2,4]

Received: 25 May 2017 / Accepted: 7 October 2017 / Published online: 16 October 2017

Abstract We investigated the changes in the East Asian summer monsoon (EASM) rainfall under global warming based on the historical and representative concentration pathway (RCP) 4.5 runs of 18 models from the fifth phase of the Coupled Model Intercomparison Project (CMIP5). Because the mechanism of rainfall changes under global warming studied in previous studies is widely based on the moisture budget decompositions (MBDs), we first evaluated the applicability of three MBDs for the changes in the EASM rainfall, which are two complete MBDs in Chou et al. (J Clim 22(8):1982–2005; Chou et al., J Clim 22(8):1982–2005, 2009) and Seager et al. (J Clim 23(17):4651–4668; Seager et al., J Clim 23(17):4651–4668, 2010), and the simplified MBD in Huang et al. (Nat Geosci 6(5):357–361; Huang et al., Nat Geosci 6(5):357–361, 2013). The results show that the simplified MBD in Huang et al. (Nat Geosci 6(5):357–361, 2013) is applicable for the EASM rainfall changes, providing an efficient way to study the EASM rainfall changes, which is used in this study. The EASM rainfall changes can be well explained by two components: the thermodynamic component due to the increase in specific humidity and the dynamic component due to the changes in EASM circulation changes. The thermodynamic component is quite robust among the models, whereas the dynamic component with the circulation changes contributes the major uncertainties of the EASM rainfall changes. Moreover, the apparent intermodel difference in the background circulation is another important source of the EASM rainfall changes. The results imply that the background and changes of the EASM circulation are the key factors for further narrowing the uncertainties of the projected EASM rainfall changes.

Keywords East Asian summer monsoon · Moisture budget · Rainfall · Global warming · Uncertainty

1 Introduction

East Asian summer monsoon (EASM) provides most of the annual mean rainfall for eastern and southern China, Korea and Japan (e.g., Endo and Kitoh 2016). Under the global warming, reliable projections of future changes in EASM rainfall are required. Most results of previous studies confirm that the EASM precipitation is likely to increase under global warming, although some uncertainties exist in the projections among present climate models (Kripalani et al. 2007; Kusunoki and Arakawa 2012; Brown et al. 2013; Chen and Sun 2013; Kitoh et al. 2013; Sooraj et al. 2015).

Several studies have investigated various changing factors influencing the changes in Asian summer monsoon rainfall. Meehl and Washington (1993) suggested that doubled CO_2 concentration heats the land faster than the ocean and increases the evaporation which results in a greater South Asian monsoon precipitation. Some studies revealed the EASM rainfall will increase under global warming, and

✉ Ping Huang
huangping@mail.iap.ac.cn

[1] State key Laboratory of Numerical Modeling for Atmospheric Sciences and Geophysical Fluid Dynamics, Institute of Atmospheric Physics, Chinese Academy of Sciences, Beijing 100029, China

[2] Laboratory for Regional Oceanography and Numerical Modeling, Qingdao National Laboratory for Marine Science and Technology, Qingdao 266237, China

[3] University of Chinese Academy of Sciences, Beijing 100049, China

[4] Center for Monsoon System Research, Institute of Atmospheric Physics, Chinese Academy of Sciences, Beijing 100190, China

attributed it to the intensification of the northwest Pacific subtropical high and the inflow of moisture from the ocean (Kimoto 2005; Kripalani et al. 2007). With the latest generation of climate models, more studies consistently revealed the increase of EASM rainfall is induced by the intensified moisture convergence and increase of evaporation, which are associated with the enhanced water vapor content under global warming (Hsu et al. 2012, 2013; Kusunoki and Arakawa 2012; Sooraj et al. 2015).

Moisture budget decomposition (MBD) is a widely used method to study the rainfall changes under global warming (Chou and Neelin 2004; Held and Soden 2006; Chou et al. 2009; Seager et al. 2010, 2012; Chou and Lan 2012; Huang et al. 2013; Ma and Xie 2013; Endo and Kitoh 2014; Huang 2014; Chen and Zhou 2015; Long and Xie 2015; Long et al. 2016; Sooraj et al. 2016). Using MBDs we can decompose the total rainfall changes into various components, which are associated with different changing factors under global warming respectively. For example, the part of rainfall changes contributed by the atmospheric specific humidity changes is often called the thermodynamic component of rainfall changes, whereas that associated with the atmospheric circulation changes is called the dynamic component. Using a MBD, Chou et al. (2009) investigated the rich-get-richer mechanism and evaluated the thermodynamic and dynamic effects over convective and subsidence regions, and Seager et al. (2010) adopted a different approach to decompose the moisture budget for evaluating the net flux of water substance. These MBDs are also used in the analyses of Asian monsoon rainfall changes (Endo and Kitoh 2014; Li et al. 2015; Sooraj et al. 2015, 2016).

The MBDs in Chou et al. (2009) and Seager et al. (2010) both are complete formulas of moisture budget. Huang et al. (2013) suggested a simplified MBD for tropical rainfall changes under global warming. The simplified MBD in Huang et al. (2013) provides a simple but efficient way to study the seasonal and spatial changes in tropical rainfall under global warming, and has been extended to study the changes in the interannual variability of tropical rainfall (Huang and Xie 2015; Huang 2016, 2017; Tedeschi and Collins 2016; Huang and Chen 2017) and to study the inter-model uncertainty of tropical rainfall changes. (Long et al. 2016). It is unclear whether the efficient MBD in Huang et al. (2013) is applicable for the EASM rainfall changes.

The present study introduces a new metric to examine the applicability of different MBDs based on the outputs of 18 models which include historical and representative concentration pathway (RCP) 4.5 runs. Our results show the simplified MBD in Huang et al. (2013) is also applicable for the EASM rainfall changes. Then, we apply the MBD in Huang et al. (2013) to study the sources of intermodel uncertainty in EASM rainfall changes, which is an important but unclear aspect of the EASM rainfall changes. The models data and methods are presented in Sect. 2. Section 3 provides the results of applicability of three MBDs and the sources of uncertainty in EASM rainfall changes. Main conclusions are shown in Sect. 4.

2 Models and methods

2.1 Models

We use the monthly outputs from 18 CMIP5 models including the historical and RCP 4.5 runs in this study. The models and their information are listed in Table 1 (Taylor et al. 2012). The present-day climatology is defined as the long-term mean during 1981–2000 in historical runs, the future climatology is defined as the mean during 2079–2098 in RCP 4.5 runs, and their difference (denoted as Δ) represents the change under global warming. The summer mean is defined as the average of June, July and August. The multi-model ensemble (MME) is defined as the average of the 18 models. All the model outputs are interpolated to $2.5^\circ \times 2.5^\circ$ gird using bilinear interpolation.

2.2 Moisture budget decompositions

Three MBDs introduced in Chou et al. (2009), Seager et al. (2010) and Huang et al. (2013) have been widely used to study the rainfall changes under global warming in previous studies (Chou and Neelin 2004; Chou et al. 2009; Seager et al. 2010, 2012; Chou and Lan 2012; Huang et al. 2013; Ma and Xie 2013; Endo and Kitoh 2014; Huang 2014; Chen and Zhou 2015; Long and Xie 2015; Long et al. 2016; Sooraj et al. 2016). In Chou et al. (2009), the estimated rainfall change $\widehat{\Delta P_C}$ can be written as:

$$\widehat{\Delta P_C} = \frac{1}{\rho_w g}\left(-\int_0^{p_s} \omega_{20}\frac{\partial \Delta q}{\partial p} - \int_0^{p_s} \Delta\omega\frac{\partial q_{20}}{\partial p} - \Delta\left(\int_0^{p_s} \boldsymbol{u}\cdot\nabla q\right)\right) + \Delta E + \text{residual}. \quad (1)$$

The estimated rainfall change $\widehat{\Delta P_S}$ in Seager et al. (2010) is written as:

$$\widehat{\Delta P_S} = \frac{1}{\rho_w g}\left(-\int_0^{p_s} \nabla\cdot\left(\boldsymbol{u}_{20}\Delta q\right)dp - \int_0^{p_s} \nabla\cdot\left(q_{20}\Delta\boldsymbol{u}\right)dp\right) + \Delta E + \text{residual}. \quad (2)$$

In Eqs. (1) and (2), P, ρ_w, p, ω, q, $\boldsymbol{u}$, and E are precipitation, the density of water, pressure, pressure velocity, specific humidity, horizontal vector wind and evaporation, respectively. The subscript s and 20 denote surface values and twentieth-century (present-day climatology) values. The first three terms on the right-hand side of Eq. (1) are

Table 1 List of the 18 CMIP5 models used in this study

Model	Institute
BCC-CSM1.1	Beijing Climate Center, China Meteorological Administration
CanESM2	Canadian Centre for Climate Modelling and Analysis
CCSM4	National Center for Atmospheric Research
CNRM-CM5	Centre National de Recherches Meteorologiques / Centre Europeen de Recherche et Formation Avancees en Calcul Scientifique
CSIRO-Mk3.6.0	Commonwealth Scientific and Industrial Research Organisation in collaboration with the Queensland Climate Change Centre of Excellence
GFDL-CM3	Geophysical Fluid Dynamics Laboratory
GFDL-ESM2G	Geophysical Fluid Dynamics Laboratory
GISS-E2-R	NASA Goddard Institute for Space Studies
GISS-E2-H	NASA Goddard Institute for Space Studies
HadGEM2-ES	Met Office Hadley Centre
INM-CM4	Institute for Numerical Mathematics
IPSL-CM5A-LR	Institut Pierre-Simon Laplace
IPSL-CM5A-MR	Institut Pierre-Simon Laplace
MIROC5	Atmosphere and Ocean Research Institute (The University of Tokyo), National Institute for Environmental Studies, and Japan Agency for Marine-Earth Science and Technology
MIROC-ESM	Japan Agency for Marine-Earth Science and Technology, Atmosphere and Ocean Research Institute (The University of Tokyo), and National Institute for Environmental Studies
MIROC-ESM-CHEM	Japan Agency for Marine-Earth Science and Technology, Atmosphere and Ocean Research Institute (The University of Tokyo), and National Institute for Environmental Studies
MRI-CGCM3	Meteorological Research Institute
NorESM1-M	Norwegian Climate Centre

thermodynamic component, dynamic component and change in horizontal moisture advection. The first two terms on the right-hand side of Eq. (2) are thermodynamic and dynamic components. The thermodynamic and dynamic components of Eq. (1) are not the same with that of Eq. (2). The Eq. (2) can be derived from Eq. (1) using the continuity equation and boundary conditions. The residuals in these two equations include mainly the transient eddy and nonlinear terms, which are negligible.

Huang et al. (2013) considered a two-layer simplification, the upper free atmosphere and the lower troposphere, and simplified the rainfall changes from Eq. (1) as follow:

$$\widehat{\Delta P_H} \sim -\frac{1}{\rho_w g}\left(\Delta\omega \cdot q_{20} + \omega_{20} \cdot \Delta q\right), \tag{3}$$

where ω, q are the pressure velocity at 500-hPa pressure level and surface specific humidity, respectively. The subscript *20* in Eq. (3) will be omitted for conciseness in the following study. The simplification of $\widehat{\Delta P_H}$ is efficient and applicable for studying the mechanism of the tropical rainfall changes (Huang et al. 2013; Huang 2014; Long et al. 2016.)

2.3 Metric for the applicability of the moisture budget decompositions

As the $\widehat{\Delta P_H}$ in Huang et al. (2013) is simplified based on the understanding of tropical rainfall changes, the estimated $\widehat{\Delta P_H}$ by the MBD of Eq. (3) could differs from the changes in rainfall changes. We call the consistency between the estimated $\widehat{\Delta P}$ by MBDs and ΔP as the applicability of the MBDs to the rainfall changes. The applicability of MBDs may depend on the locations and seasons. A metric, the local correlation coefficient between the $\widehat{\Delta P}$ by MBDs and ΔP, is defined as follows to evaluate their applicability in different locations and seasons. First, we have four grids around a given grid on the north, south, west and east, respectively. We select the given grid with the four grids around it in the 18 CMIP5 models to get a 90-member series of one variable for the given grid. Finally, we can calculate the correlation coefficient between the 90-member series of ΔP and that of estimated rainfall changes by the MBD for the given grid. The local correlation coefficient is used to quantify the applicability of one MBD on a given grid. The local correlation coefficient is calculated for the three MBDs, $\widehat{\Delta P_C}$, $\widehat{\Delta P_S}$, and $\widehat{\Delta P_H}$.

2.4 Intermodel uncertainty

In this study, the uncorrected sample standard deviation (SD) of changes among the models is used to quantify the absolute intermodel spread of changes. Further, the signal-to-noise ratio (SNR) to measure the robustness of the MME changes is defined as the ratio of the MME to the intermodel standard deviation of a variable, i.e., SNR = Δ/σ, where Δ denotes the MME of changes and σ denotes the intermodel standard deviation of changes in the 18 models. The SNR is useful to quantify the robustness of changes (Long et al. 2016; Huang 2017).

3 Results

3.1 Applicability of three moisture budget decompositions

Figure 1a, b show the annual-mean and summer-mean ΔP in the MME of 18 CMIP5 models under RCP 4.5 runs to compare with the estimated rainfall changes, $\widehat{\Delta P_C}$, $\widehat{\Delta P_S}$, and $\widehat{\Delta P_H}$. The annual-mean ΔP (Fig. 1a) is primitively positive over the equatorial Pacific Ocean with a hook-like pattern, and weakly positive over the northern Indian Ocean, India Peninsula, Southeast Asia and East Asia. During the summer (Fig. 1b), the pattern of summer-mean ΔP shifts northward along with the shift of climatological rainfall as a result of the wet-get-wetter mechanism (Huang et al. 2013).

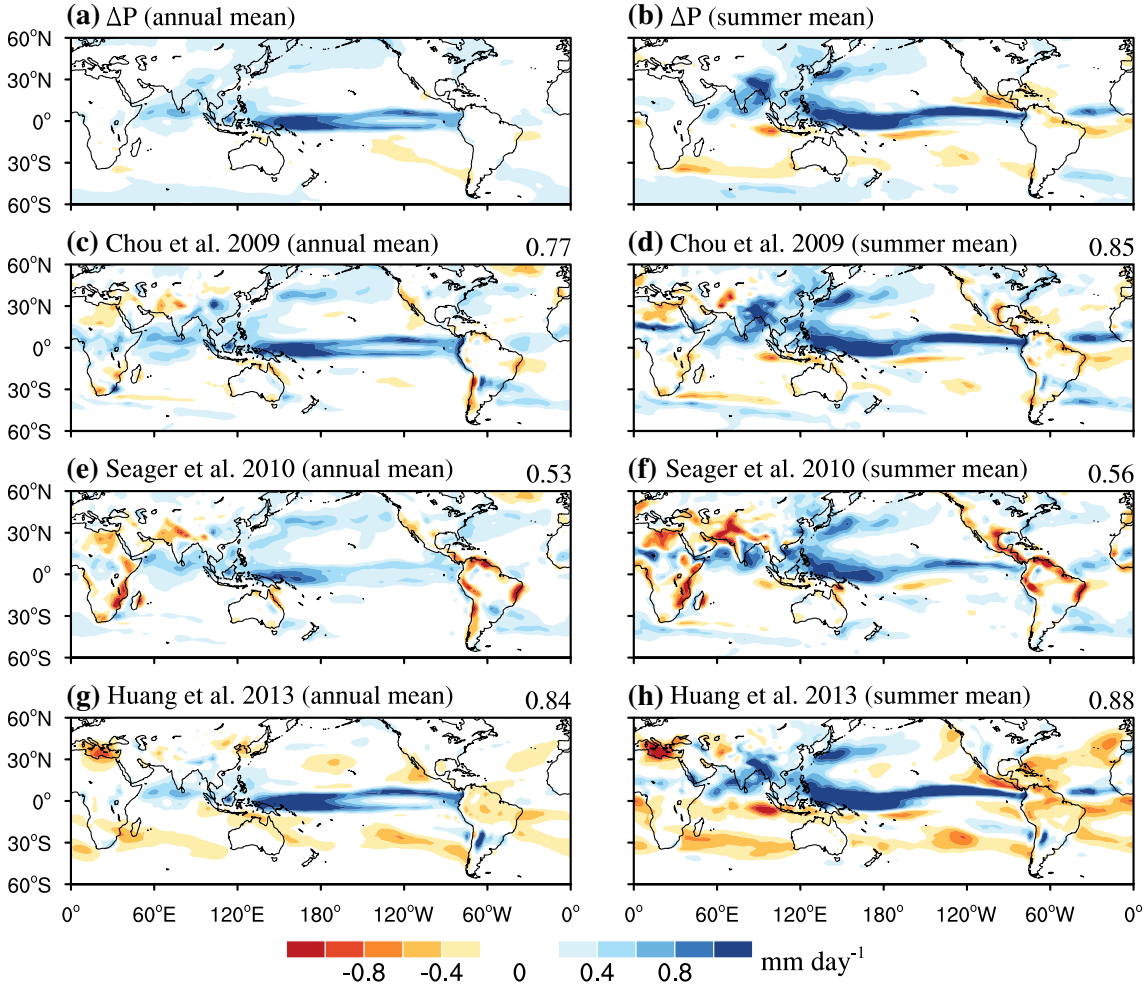

Fig. 1 **a** The annual-mean and **b** summer-mean rainfall change in the MME of the 18 CMIP5 models under the RCP 4.5 scenario. And annual-mean (**c, e, g**) and summer-mean (**d, f, h**) ΔP calculated by the right sides of the moisture budget decomposition Eqs. (1)–(3), which are the method in Chou et al. (2009), Seager et al. (2010) and Huang et al. (2013) respectively. The pattern correlation coefficients between the direct rainfall changes (**a, b**) and the moisture budget calculations based on Eqs. (1)–(3) are shown at the top-right corner of the each panel (**c**–**h**)

Figure 1c–h show the annual mean and summer mean of the three MBDs $\widehat{\Delta P_C}$, $\widehat{\Delta P_S}$, and $\widehat{\Delta P_H}$. In general, they all reproduce the primary characteristics of the spatial patterns of ΔP in the annual mean and boreal summer mean. The pattern correlation coefficients of the ΔP with the estimated rainfall changes $\widehat{\Delta P_C}$, $\widehat{\Delta P_S}$, and $\widehat{\Delta P_H}$, are all significant, which are showed at the top-right corner of each panel (c, d, e, f, g, h) in Fig. 1. The $\widehat{\Delta P_H}$ (Fig. 1g,h) consists with the ΔP (Fig. 1a,b) best in them with the largest pattern correlation coefficient. The $\widehat{\Delta P_H}$ shows almost the same pattern with the $\widehat{\Delta P_C}$ (Fig. 1c, d). For the $\widehat{\Delta P_S}$ (Fig. 1e, f), however, there are two differences compared with ΔP, the $\widehat{\Delta P_S}$ is underestimated over the ocean, and there are large biases of $\widehat{\Delta P_S}$ in regions of topography such as Himalayas and Andes (Seager et al. 2010). The pattern correlation coefficient between the ΔP and the $\widehat{\Delta P_S}$ is lower than the other two MBDs.

To further illustrate the applicability of the $\widehat{\Delta P_C}$ and $\widehat{\Delta P_H}$, we calculate the local correlation coefficient of $\widehat{\Delta P_C}$ and $\widehat{\Delta P_H}$ with ΔP, respectively (Fig. 2). The local correlation coefficients are higher than 0.75 over the tropical ocean and decrease immediately when they get close to the land. High correlation coefficients are also found over the tropical land with the climatological precipitation greater than 4 mm day^{-1} in the annual mean and the summer mean. In boreal summer, the distribution of high climatological precipitation shift northward (Fig. 2b, d). As a result, the high correlation coefficients are also shift northward. Although the $\widehat{\Delta P_C}$ is a complete formula and the $\widehat{\Delta P_H}$ is simplified for

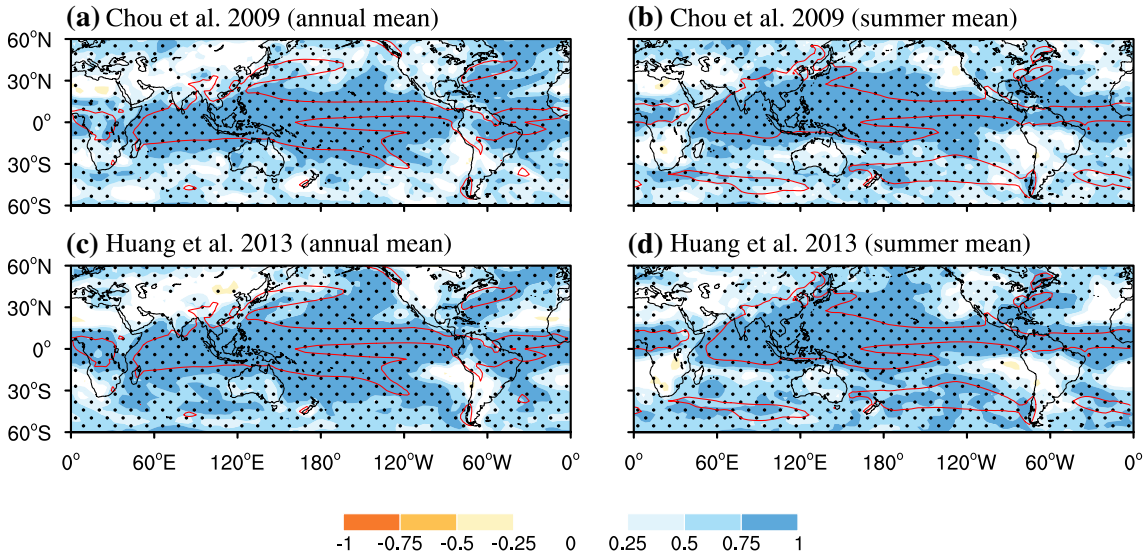

Fig. 2 The defined 5-point local correlation coefficient (shaded) of the ΔP with the estimated $\widehat{\Delta P_C}$ (**a, b**) and $\widehat{\Delta P_H}$ (**c, d**), respectively, for the (**a, c**) annual mean and the (**b, d**) summer mean. Red curves are the 4 mm day^{-1} contour of the climatological rainfall. Stippling indicates where the correlation coefficient passes the student t test at the 95% confidence level

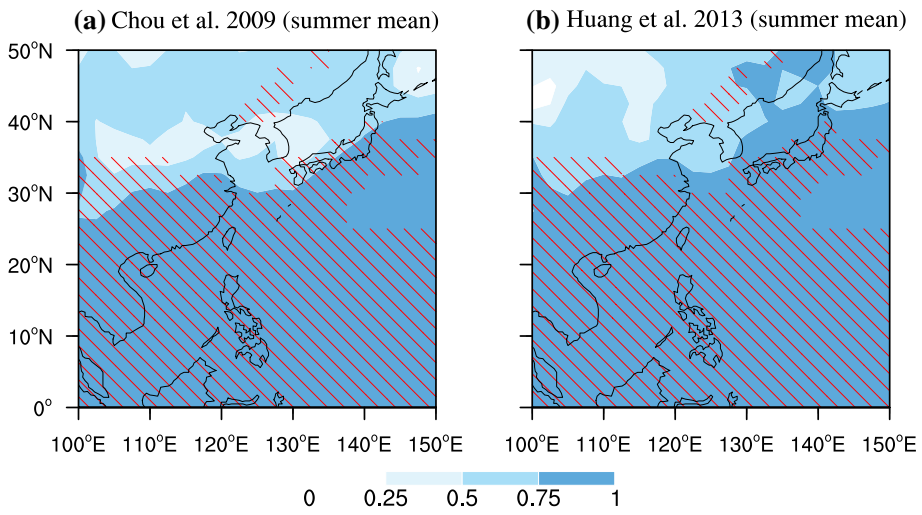

Fig. 3 As in Fig. 2b, d, but especially for the EASM area. Red hatching denotes the summer-mean rainfall climatology greater than 4 mm day^{-1}

the tropical rainfall, there is no apparent difference between their applicability from 60°S to 60°N (Fig. 2). Especially, the high applicability of $\widehat{\Delta P_H}$ is also shift northward along with the high climatological rainfall to the mid-latitude of the northern hemisphere in boreal summer (Fig. 2d).

Figure 3 emphasizes the applicability of the two MBDs over the EASM region in boreal summer. The applicability of $\widehat{\Delta P_C}$ and $\widehat{\Delta P_H}$ is almost the same in this situation. Their local correlation coefficients with ΔP are larger than 0.75 in the major EASM regions. This result shows the efficient MBD $\widehat{\Delta P_H}$ is applicable to study the changes in EASM rainfall for the MME.

Because an important application of MBDs is to study the sources of the intermodel uncertainty of rainfall changes, we further illustrate the applicability of the $\widehat{\Delta P_H}$ in the individual models (Fig. 4). Consistent with previous studies (Kusunoki and Arakawa 2012; Chen and Sun 2013; Kitoh et al. 2013; Sooraj et al. 2015), the EASM rainfall changes show large intermodel uncertainty. However, the estimated $\widehat{\Delta P_H}$ reproduce the EASM rainfall changes very well in each model. The pattern correlation coefficients between them in all models are significant. The high applicability of $\widehat{\Delta P_H}$ in the MME and the individual models suggests that the efficient $\widehat{\Delta P_H}$ in Huang et al. (2013) can also be applied to study the EASM rainfall changes.

3.2 The sources of the intermodel uncertainty in the EASM rainfall changes

The main sources of uncertainty in the EASM rainfall changes could include the model uncertainty, scenario uncertainty, and the internal variability of the climate system (Hawkins and Sutton 2009). Among the three sources, the model uncertainty will increase much larger than the internal variability in the projection for the end of twenty-first century, when the only one scenario, for example the RCP 4.5 in the present study, is considered (Hawkins and Sutton 2009; Kent et al. 2015). To further narrow the intermodel uncertainty, we apply the simplified MBD in Huang et al. (2013) to investigate the sources of the intermodel uncertainty in the EASM rainfall changes.

Figure 5 shows the thermodynamic and dynamic components of ΔP decomposed by the MBD of Huang et al. (2013), whose sum is shown in Fig. 5c. The thermodynamic component (Fig. 5a) is positive over EASM region, but the sign of dynamic component (Fig. 5b) varies over EASM region. The magnitudes of the two components are close. Figure 6 displays the intermodel SD of the two components in the 18 models and the SNR of the two components in the MME. The SD of the thermodynamic component (Fig. 6a), almost less than 0.6, is much smaller than that of the dynamic component (Fig. 6b). The sign agreement test and the SNR of thermodynamic component (Fig. 6c) is almost larger than 1, showing that the thermodynamic component of ΔP is quite robust among the models. In contrast, the dynamic dominates the major uncertainty of ΔP.

To further investigate the contributions of each part in these two components, respectively, we separate their SD to the contribution of each component. The SD of the thermodynamic component, $\omega\Delta q$, is separated as $\boldsymbol{\sigma}(\Delta q)|\bar{\omega}|$ and $\boldsymbol{\sigma}(\omega)\left|\overline{\Delta q}\right|$, where the $\boldsymbol{\sigma}(\cdot)$indicates the intermodel SD among the models and the overbar indicates MME of the models (Huang 2017). Similarly, the SD of the dynamic component, $\Delta\omega q$, is separated as $\boldsymbol{\sigma}(q)\left|\overline{\Delta\omega}\right|$ and $\boldsymbol{\sigma}(\Delta\omega)|\bar{q}|$. The SD due to $\Delta\omega$ is largest (the color bar in Fig. 7d differs from the others) among the four terms, whereas the SD due to present-day surface specific humidity is smallest. For the two terms of the thermodynamic component, the SD due to Δq is smaller than that due to ω, indicating that the dominant uncertainty source of thermodynamic component is the historical ω although ω is not a projected variable.

The SD and SNR (Fig. 8) of the four variables reveals that the circulation changes $\Delta\omega$ are the largest source of the model uncertainty in future precipitation changes, the q is negligible, Δq is consistently projected by the models, and the background of circulation ω is another important factor to the source of the intermodel uncertainty. This result indicates that improving the projection of EASM circulation changes is the most important way to improve the robustness of EASM rainfall changes, and using observed climatological ω to constrain the thermodynamic part of EASM rainfall changes could be valuable to the projection of ΔP.

4 Conclusions and discussions

The EASM rainfall changes are an important issue of the climate changes for the EASM regions under global warming. The EASM rainfall changes projected by the CMIP5 models show large intermodel uncertainty. What are the most important sources of the intermodel uncertainty of the EASM rainfall changes and how to reduce them are unclear. To study the EASM rainfall changes, the moisture budget decompositions were a widely used method. This study first investigated the applicability of three MBDs to the EASM rainfall changes, which including two complete MBDs of Chou et al. (2009) and Seager et al. (2010), and a simplified MBD of Huang et al. (2013). Then we applied the MBD of Huang et al. (2013) to investigate the sources of intermodel uncertainty of EASM rainfall changes under global warming projected by 18 CMIP5 models in the historical and RCP 4.5 runs.

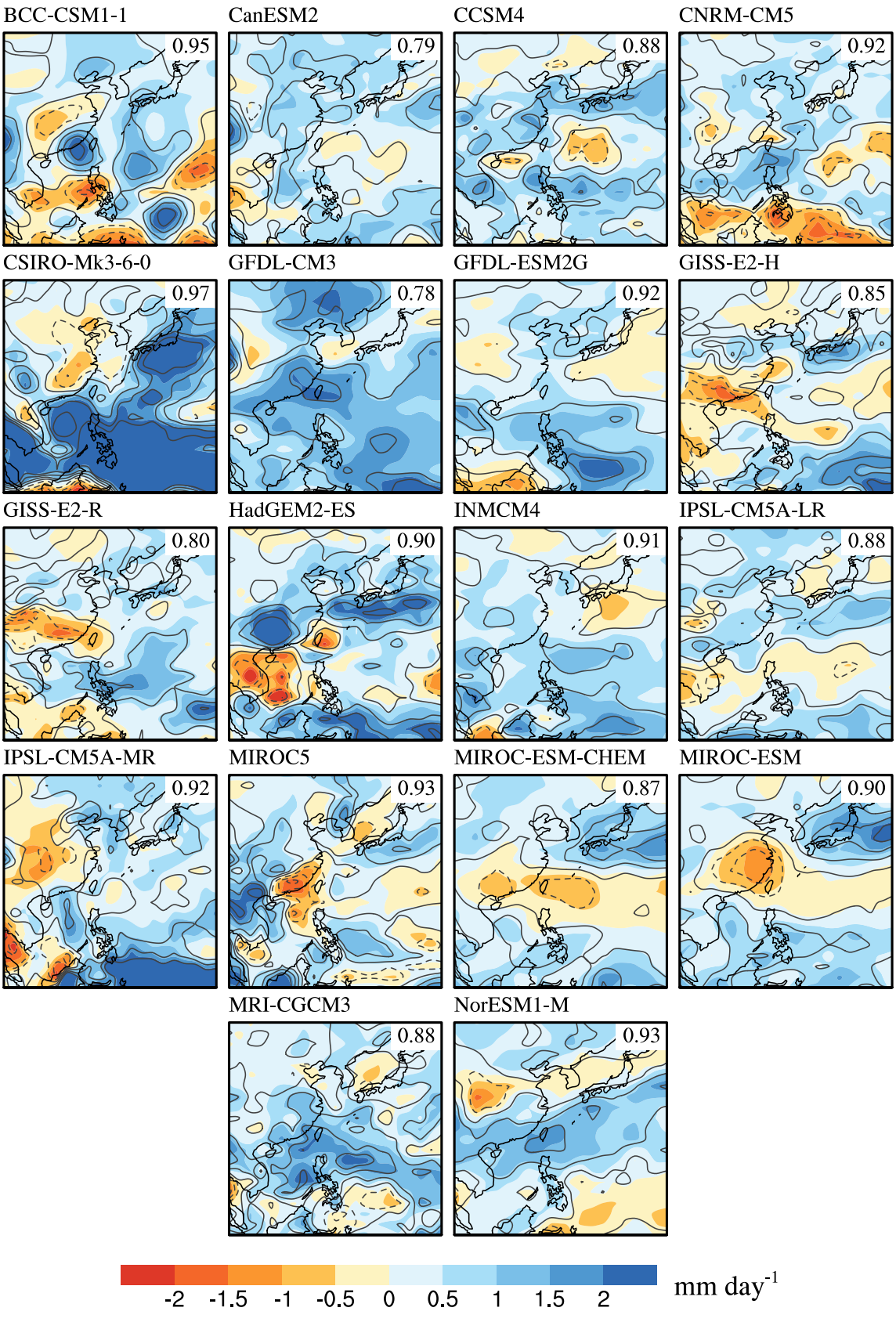

Fig. 4 Summer-mean ΔP (shaded) and $\widehat{\Delta P_H}$ (contours; contour interval 1 mm day^{-1} and negative contours dashed) of the 18 CMIP5 models. The pattern correlation coefficient between ΔP and $\widehat{\Delta P_H}$ is shown at the top-right corner of each panel

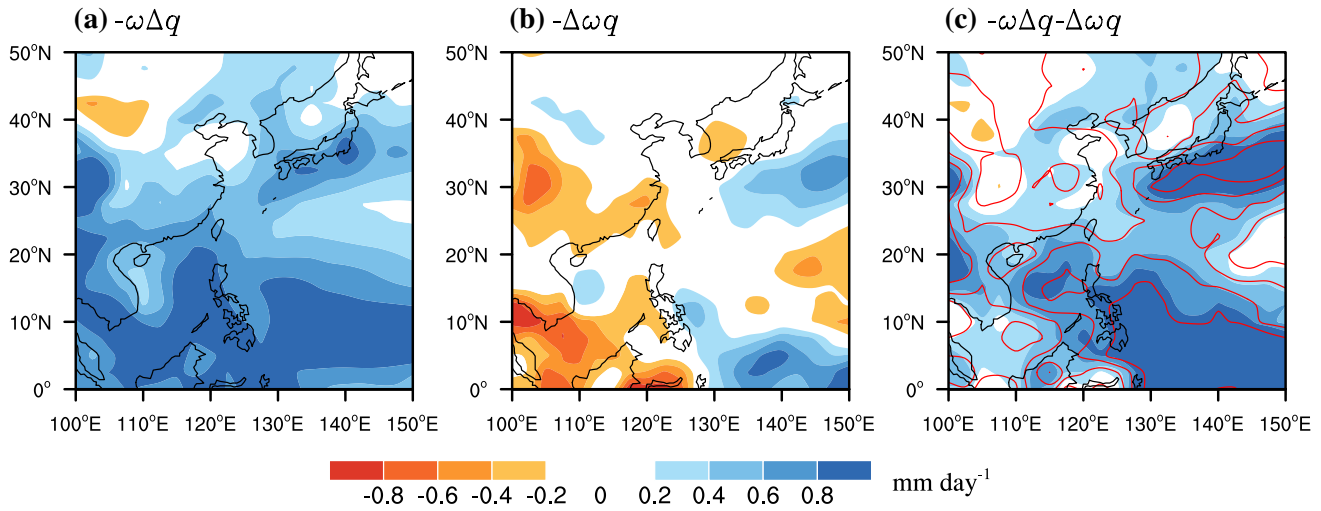

Fig. 5 The summer-mean **a** thermodynamic ($-\omega\Delta q$) and **b** dynamic ($-\Delta\omega q$) components of in the estimated rainfall changes in Huang et al. (2013) and **c** their sum of them. Red curves in **c** are the contours of ΔP, in which contour interval is 0.2 mm day^{-1} and negative contours are dashed

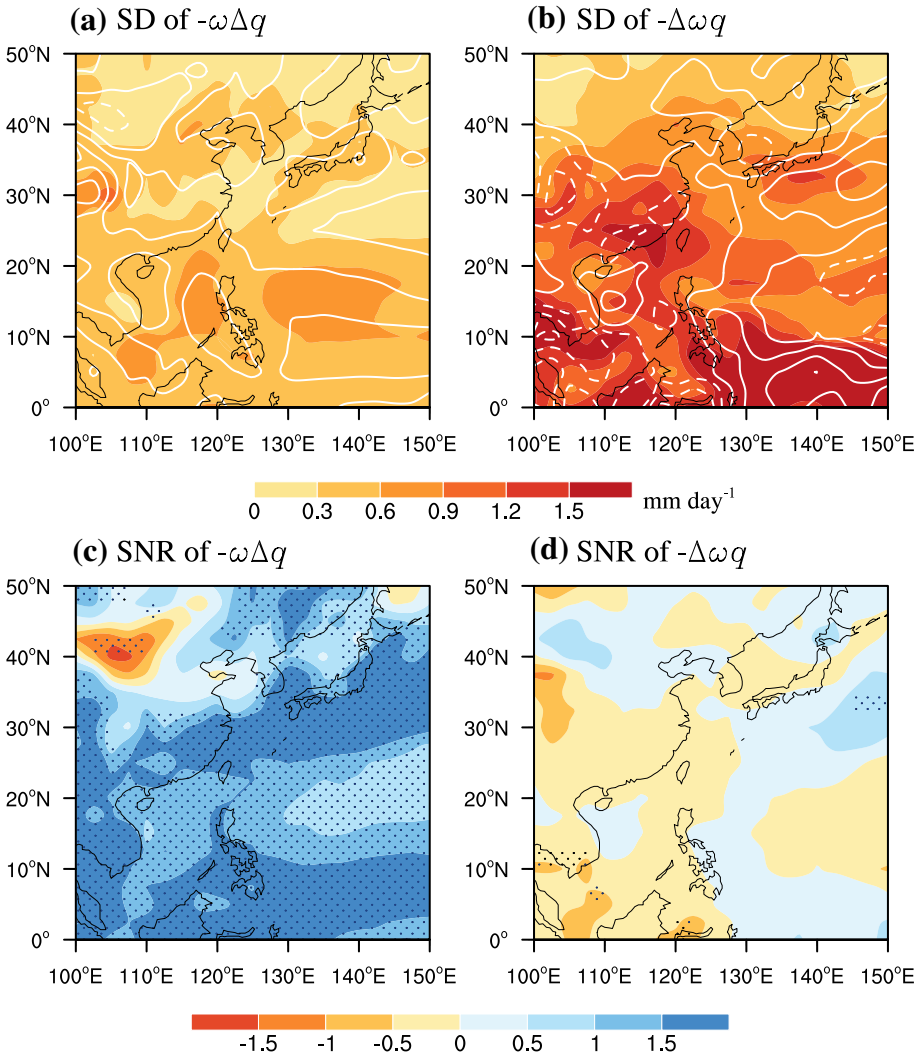

Fig. 6 The **a, b** SD and **c, d** SNR of the thermodynamic ($-\omega\Delta q$) and dynamic ($-\Delta\omega q$) components. Contours in **a, b** are the MME changes in the thermodynamic and dynamic components (contour interval 0.3 mm day^{-1} and negative contours dashed). Stippling in **c, d** indicates that more than 70% models agree on the sign of the MME changes

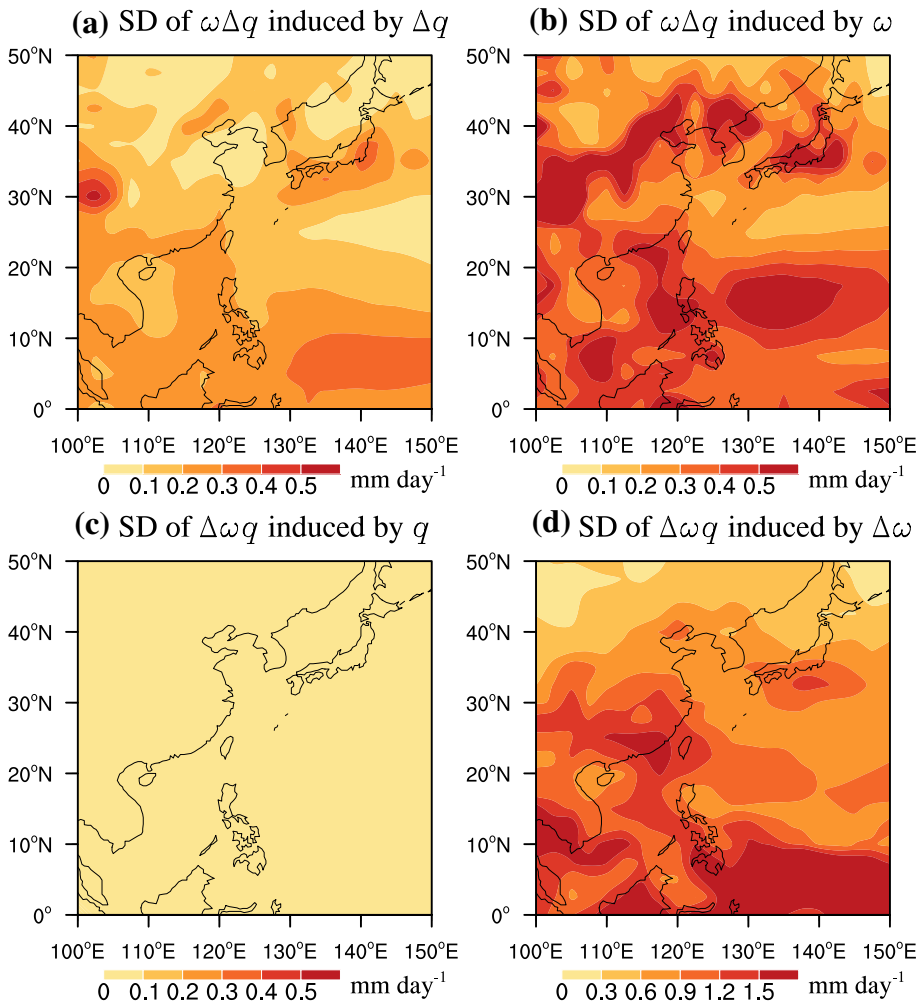

Fig. 7 The SD of the thermodynamic ($-\omega\Delta q$) components contributed by the SD of **a** Δq and **b** ω. The SD of the dynamic ($-\Delta\omega q$) components contributed by the SD of **c** q and **d** $\Delta\omega$. Note that the color bar in **d** differs from the others

In general, the applicability of the MBD of Seager et al. (2010) is weaker than the MBDs of Seager et al. (2010) and Huang et al. (2013). The applicability of $\widehat{\Delta P_C}$ is very close to that of $\widehat{\Delta P_H}$, although $\widehat{\Delta P_H}$ is simplified for the tropical rainfall. The applicability of the two MBDs are quite high over the tropical ocean and the regions with the climatological rainfall larger than 4 mm day^{-1}. Following the seasonal shift of the climatological rainfall, the applicability of the two MBDs also show apparent seasonal shift to the summer hemisphere. For the EASM regions, the applicability of $\widehat{\Delta P_H}$, a simplified MBD, is similar to that of the complete MBD of Chou et al. (2009) in boreal summer. The simplified MBD, $\widehat{\Delta P_H}$, provides an efficient way to study the various aspects of the EASM rainfall changes.

In this study, we applied the MBD $\widehat{\Delta P_H}$ to investigate the source of the intermodel uncertainty in the EASM rainfall changes. The total EASM rainfall changes were decomposed into the thermodynamic and dynamic component, which are induced by the increase in specific humidity and the EASM circulation changes, respectively. By analyzing the intermodel standard deviation and signal-to-noise ratio, we conclude that the EASM circulation changes is the largest source of the intermodel uncertainty consistent with the previous study (Kent et al. 2015), suggesting that the projection of EASM circulation changes is the key to improve the projection of EASM rainfall changes. On the other hand, the background circulation is also an important source of the intermodel uncertainty of the EASM rainfall changes. As the background circulation of model can be compared with observations, this result implies that the observational constraint method is potential to correct the intermodel spread of the thermodynamic component in the EASM rainfall changes.

The present study attributes the key source of intermodel uncertainty of the EASM rainfall changes to the EASM circulation change. An analysis for the seasonal tropical precipitation change also attributes the primary driver of intermodel uncertainty of the seasonal tropical ΔP to the spatial shifts in tropical circulation (Kent et al. 2015). However, the causes of the large uncertainty of the circulation changes is unclear yet in further attributions

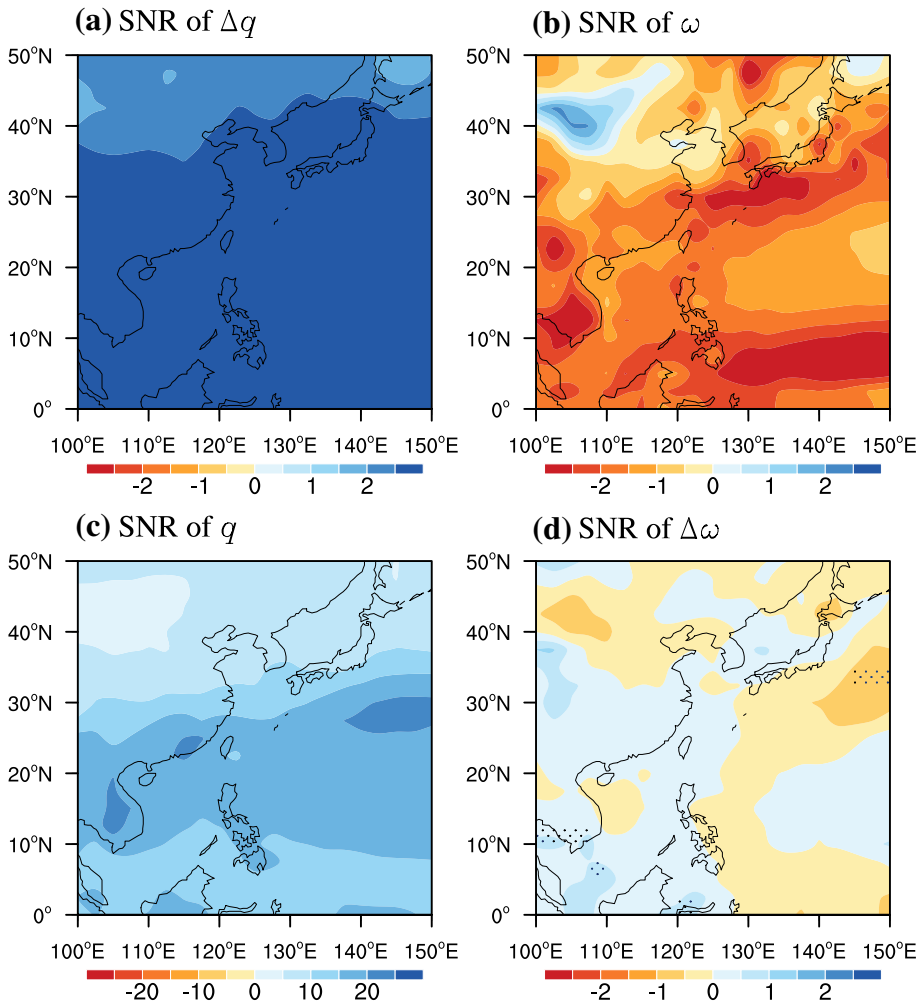

Fig. 8 The SNR of **a** Δq, **b** ω, **c** q, **d** $\Delta\omega$. Stippling in **d** indicates that more than 70% models agree on the sign of the MME changes

(Shepherd 2014). Under global warming, the EASM circulation is likely to weaken and shift northward due to reduction in the meridional gradient of temperature over the Asian region (Ueda et al. 2006; Sooraj et al. 2015). The land–ocean contrast is an important mechanism for the monsoon circulation changes (Fasullo 2012). Kamae et al. (2014) reveals that the increasing land–ocean contrast in boreal summer over East Asia is explained by the CO_2-induced warming but not the sea surface temperature warming. However, the intermodel uncertainty of circulation changes may be associated with the sea surface temperature warming pattern over the tropical ocean (Ma and Xie 2013; Brown et al. 2016). He et al. (2014) suggest that the impact of the direct effect of radiative cooling on the circulation changes is larger than that of the sea surface temperature warming pattern over most regions, consistent with the conclusion in Bony et al. (2013) and Kamae et al. (2014). Therefore, the uncertainty of the EASM circulation could involve multiply important sources, which could be the key point for the EASM changes under global warming in further research.

Acknowledgements This work is supported by the National Basic Research Program of China (2014CB953904), the Natural Science Foundation of China (41425019 and 41661144016), the public science and technology research funds projects of ocean (201505013) and the Youth Innovation Promotion Association of CAS. We acknowledge the World Climate Research Programme's Working Group on Coupled Modeling, which is responsible for CMIP5, and the climate modeling groups (listed in Table 1) for producing and making available their model output.

References

Bony S, Bellon G, Klocke D, Sherwood S, Fermepin S, Denvil S (2013) Robust direct effect of carbon dioxide on tropical circulation and regional precipitation. Nat Geosci 6(6):447–451

Brown JR, Colman RA, Moise AF, Smith IN (2013) The western Pacific monsoon in CMIP5 models: Model evaluation and projections. J Geophys Res Atmos 118(22):12,458–12,475

Brown JR, Moise AF, Colman R, Zhang H (2016) Will a warmer world mean a wetter or drier Australian monsoon? J Clim 29(12):4577–4596

Chen H, Sun J (2013) Projected change in East Asian summer monsoon precipitation under rcp scenario. Meteorol Atmos Phys 121(1–2):55–77

Chen XL, Zhou TJ (2015) Distinct effects of global mean warming and regional sea surface warming pattern on projected uncertainty in the South Asian summer monsoon. Geophys Res Lett 42(21):9433–9439

Chou C, Lan C-W (2012) Changes in the annual range of precipitation under global warming. J Clim 25(1):222–235

Chou C, Neelin JD (2004) Mechanisms of global warming impacts on regional tropical precipitation. J Clim 17:2688–2701

Chou C, Neelin JD, Chen C-A, Tu J-Y (2009) Evaluating the "rich-get-richer" mechanism in tropical precipitation change under global warming. J Clim 22(8):1982–2005

Endo H, Kitoh A (2014) Thermodynamic and dynamic effects on regional monsoon rainfall changes in a warmer climate. Geophys Res Lett 41(5):1704–1711

Endo H, Kitoh A. In: de Carvalho LMV (2016) Projecting changes of the Asian summer monsoon through the twenty-first century. In: Jones C (ed) The monsoons and climate change: Observations and modeling. Springer International Publishing, Cham, pp 47–66

Fasullo J (2012) A mechanism for land–ocean contrasts in global monsoon trends in a warming climate. Clim Dyn 39(5):1137–1147

Hawkins E, Sutton R (2009) The potential to narrow uncertainty in regional climate predictions. Bull Am Meteorol Soc 90(8):1095–1107

He J, Soden BJ, Kirtman B (2014) The robustness of the atmospheric circulation and precipitation response to future anthropogenic surface warming. Geophys Res Lett 41(7):2614–2622

Held IM, Soden BJ (2006) Robust responses of the hydrological cycle to global warming. J Clim 19:5686–5699

Hsu P-c, Li T, Luo J-J, Murakami H, Kitoh A, Zhao M (2012) Increase of global monsoon area and precipitation under global warming: A robust signal? Geophys Res Lett 39(6):L06701

Hsu P-c, Li T, Murakami H, Kitoh A (2013) Future change of the global monsoon revealed from 19 CMIP5 models. J Geophys Res Atmos 118:1247–1260

Huang P (2014) Regional response of annual-mean tropical rainfall to global warming. Atmos Sci Lett 15(2):103–109

Huang P (2016) Time-varying response of ENSO-induced tropical Pacific rainfall to global warming in CMIP5 models. Part I: Multimodel ensemble results. J Clim 29(16):5763–5778

Huang P (2017) Time-varying response of ENSO-induced tropical Pacific rainfall to global warming in CMIP5 models. Part II: Intermodel uncertainty. J Clim 30(2):595–608

Huang P, Chen D (2017) Enlarged asymmetry of tropical Pacific rainfall anomalies induced by El Niño and La Niña under global warming. J Clim 30(4):1327–1343

Huang P, Xie S-P (2015) Mechanisms of change in ENSO-induced tropical Pacific rainfall variability in a warming climate. Nat Geosci 8(12):922–926

Huang P, Xie S-P, Hu K, Huang G, Huang R (2013) Patterns of the seasonal response of tropical rainfall to global warming. Nat Geosci 6(5):357–361

Kamae Y, Watanabe M, Kimoto M, Shiogama H (2014) Summertime land–sea thermal contrast and atmospheric circulation over East Asia in a warming climate—part II: Importance of CO2-induced continental warming. Clim Dyn 43(9–10):2569–2583

Kent C, Chadwick R, Rowell DP (2015) Understanding uncertainties in future projections of seasonal tropical precipitation. J Clim 28(11):4390–4413

Kimoto M (2005) Simulated change of the east Asian circulation under global warming scenario. Geophys Res Lett 32 (16)

Kitoh A, Endo H, Krishna Kumar K, Cavalcanti IFA, Goswami P, Zhou T (2013) Monsoons in a changing world: A regional perspective in a global context. J Geophys Res Atmos 118(8):3053–3065

Kripalani RH, Oh JH, Chaudhari HS (2007) Response of the East Asian summer monsoon to doubled atmospheric CO2: Coupled climate model simulations and projections under IPCC AR4. Theor Appl Climatol 87(1–4):1–28

Kusunoki S, Arakawa O (2012) Change in the precipitation intensity of the East Asian summer monsoon projected by CMIP3 models. Clim Dyn 38(9–10):2055–2072

Li XQ, Ting MF, Li CH, Henderson N (2015) Mechanisms of Asian summer monsoon changes in response to anthropogenic forcing in CMIP5 models. J Clim 28(10):4107–4125

Long S-M, Xie S-P (2015) Intermodel variations in projected precipitation change over the North Atlantic: Sea surface temperature effect. Geophys Res Lett 42(10):4158–4165

Long S-M, Xie S-P, Liu W (2016) Uncertainty in tropical rainfall projections: Atmospheric circulation effect and the ocean coupling. J Clim 29(7):2671–2687

Ma J, Xie S-P (2013) Regional patterns of sea surface temperature change: A source of uncertainty in future projections of precipitation and atmospheric circulation. J Clim 26(8):2482–2501

Meehl GA, Washington WM (1993) South Asian summer monsoon variability in a model with doubled atmospheric carbon dioxide concentration. Science 260:1101–1104

Seager R, Naik N, Vecchi GA (2010) Thermodynamic and dynamic mechanisms for large-scale changes in the hydrological cycle in response to global warming. J Clim 23(17):4651–4668

Seager R, Naik N, Vogel L (2012) Does global warming cause intensified interannual hydroclimate variability? J Clim 25(9):3355–3372

Shepherd TG (2014) Atmospheric circulation as a source of uncertainty in climate change projections. Nat Geosci 7(10):703–708

Sooraj KP, Terray P, Mujumdar M (2015) Global warming and the weakening of the Asian summer monsoon circulation: Assessments from the CMIP5 models. Clim Dyn 45(1–2):233–252

Sooraj KP, Terray P, Xavier P (2016) Sub-seasonal behaviour of Asian summer monsoon under a changing climate: Assessments using CMIP5 models. Clim Dyn 46(11–12):4003–4025

Taylor KE, Stouffer RJ, Meehl GA (2012) An overview of CMIP5 and the experiment design. Bull Am Meteorol Soc 93(4):485–498

Tedeschi RG, Collins M (2016) The influence of ENSO on South American precipitation: Simulation and projection in CMIP5 models. Int J Climatol. doi:10.1002/joc.4919

Ueda H, Iwai A, Kuwako K, Hori ME (2006) Impact of anthropogenic forcing on the Asian summer monsoon as simulated by eight GCMs. Geophys Res Lett 33(6):L06703